



A High Efficiency and High Step Up Solar Fed Coupled Inductor Converter for PMDC Motor Drives

G. Arthiraja¹, M. Ammal Dhanalakshmi², P.Pravina³, M. Sasikumar⁴

PG Scholar, Department of Power Electronics and Drives, Jeppiaar Engineering College, Chennai, India^{1,2}

Asst. Prof., Department of EEE, Jeppiaar Engineering College, Chennai, India³

Professor & Head, Department of EEE, Jeppiaar Engineering College, Chennai, India⁴

Abstract—An efficient DC/DC converter with soft switching topology is proposed in this paper. This converter efficiently utilizes the energy stored in the passive elements to improve the performance of the Boost converter. With the interest in the utilization of renewable energy resources that is available in huge amount in our country, the proposed converter is powered by the solar photovoltaic system. And further, the proposed converter is applied for drive applications wherein the Permanent Magnet DC motor (PMDC) is used to drive the load. In addition, the semiconductor switch used in the proposed system is controlled by the Triangular Pulse Width Modulation (TPWM) Strategy. And also, the switches with low on state resistance are used to reduce the conduction losses. The design and modeling of the proposed DC/DC converter is simulated by using MATLAB tool and the results are analyzed and discussed in the fore coming chapters.

Keywords—DC/DC converter, Drive applications, triangular pulse width modulation, coupled inductor.

I. INTRODUCTION

With the increasing demand for high voltage in the industrial applications, efficient DC/DC converter with high step up voltage gain is widely used. This need proliferates in designing an efficient DC/DC converter with reduced components, filter size and cost which will lead the converter for easy public marketing. Usually, the boost DC/DC converter operates at high step up voltage gain at high duty cycle. But unfortunately the passive elements present in the circuit become an obstacle for achieving high step up voltage gain. Hence in order to improve the efficiency of the converter, energy stored in the passive components like capacitor and the coupled inductor [1], [2], must be efficiently utilized by the

system. Thus this paper proposes a transformerless high gain step up DC/DC converter [3]–[6] with practical and economical considerations.

Permanent Magnet DC (PMDC), [7] motors are widely used in a range of applications, from battery powered devices like wheelchairs and power tools, to conveyors and door openers, welding equipment, X-ray and tomographic systems, and pumping equipments. These motors have the ability to produce high torque at low speed. Its design yields a smaller, lighter, and energy efficient motor. The PM motor's field has a high reluctance (low permeability) that eliminates significant armature interaction. This high reluctance yields a constant field, permitting linear operation over the motor's entire speed-torque range. Applications such as amusement drives, pump drives etc. requires high DC voltage.

In Triangular PWM, the output voltage is controlled by varying the duty cycle. The duty cycle in turn is controlled by varying the reference and the carrier wave signals. In this method a constant reference signal V_{ref} is compared with the triangular carrier wave signal. The peak magnitude is limited by the peak carrier wave signal. Among all renewable energy sources, solar power systems [8]–[10] attract more attention because they provide excellent opportunity to generate electricity while greenhouse emissions are reduced. The only way of generating electricity from solar energy will be PV cells or panels. Temperature, insulation, Spectral characteristics of sunlight, dirt, shadow etc., are the main factors to be considered for the efficiency of the solar cells.

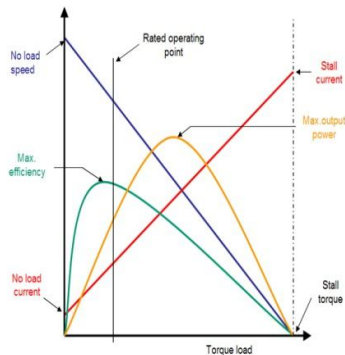


Fig.1 Performance curve of PMDC motor

The PV cells are made up of silicon, which is also used in computer "chips". The radiation produced from the sun will be converted into direct current (DC) by this Photovoltaic process. This point is known as maximum power point (MPP). The MPPT [11] is the efficient way to track the maximum available output power of the PV system.

The performance curve of PMDC motor is shown in Fig. 1. In operation, with a constant armature voltage, as speed decreases, available torque increases. Speed is controlled by varying the voltage applied to the armature. PMDC motors use a mechanical commutation scheme to switch current to the armature winding. Feedback devices sense motor speed and send this information to the control to vary its output voltage up or down to keep speed at or near the set value.

II. PROPOSED CIRCUIT DESCRIPTION

A. Circuit Configuration

The circuit configuration of the proposed converter is shown in Fig.2. The main components of the proposed circuit are main switch S, clamping capacitor C1, clamping diode D1, one coupled inductor N_p and N_s , two capacitors C2 and C3, two diodes D2 and D3, Output capacitor C_o , and Output diode D_o . This circuit is powered by a PV panel and it drives a PMDC motor load. The equivalent circuit model also includes leakage inductance L_k and magnetizing inductance L_M .

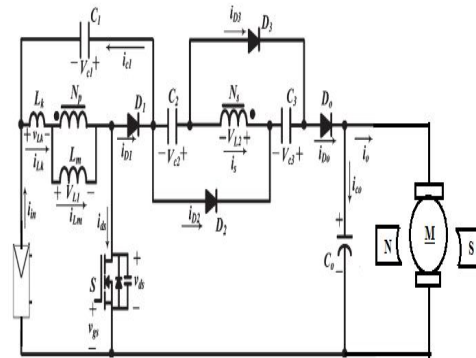


Fig.2 Circuit Configuration of the Proposed Converter

The leakage energy stored in the coupled inductor is recycled to the capacitor and hence the voltage stress across the switch is reduced. This feature of the proposed converter increases the performance and thus the efficiency of the converter.

B. Operating principle of the Proposed Converter

When switch is ON, V_{in} charges L_M and in turn the secondary side of the coupled inductor. Similarly, when the switch is OFF, the energy stored in L_M is discharged through the secondary side of the coupled inductor. In order to reduce the voltage across the switch S, the capacitors C2 and C3 discharge in series whereas they charge in parallel during the turn OFF and turn ON process respectively.

C. Continuous Current Mode operation of the proposed converter

There are five operating modes in each switching cycle. Each operating mode is discussed below in detail.

Mode I : In this mode, S is ON. As mentioned in the previous topic, V_{in} charges L_M and the secondary side of the coupled inductor. Thus the secondary side current i_s charges C2 and turns ON the diodes D2, D3 and the capacitor C3. The output capacitor C_o supplies the load. The current flow is shown in Fig.3(a). The expression for the input voltage can be written as,

$$V_{in} = V_{L_k} + V_{L_M} \quad (1)$$

Mode II : During this interval, S remains ON, the source current charges L_M and also travels to the secondary side through the coupled inductor. A part of the source current takes the path of capacitors C1, C2 and C3. All the three capacitors discharge the stored energy in series to the load by turning ON the output diode D_o . Fig.3(b) shows the current flow direction.

Mode III : As soon as, the three capacitors completely discharge to the output voltage, S is turned OFF. The source current thus flows through the coupled inductor, L_M , and the parasitic capacitor C_{ds} of the switch S. Thus ZVS is achieved for the switch S. The output capacitor C_o supplies the load. Fig.3(c) represents this mode.

Mode IV : In this mode, the moment the parasitic capacitor C_{ds} gets fully charged, the source current now flows through the L_M , coupled inductor, D_1 , C_2, C_3, D_0 and the load. Further the energy stored in the leakage inductor L_k is recycled through the clamping capacitor C_1 . The circuit representation for the above explanation is shown in Fig.3(d).

Mode V : During this interval, the supply voltage is detached. The recycled energy of L_k flows through L_M . The current flowing through also flows through the coupled inductor. This charges the capacitors C_2 and C_3 in parallel. The secondary current also flows through the diodes D_2 and D_3 . C_o supplies the load. At the end of this mode switch S turns ON and the cycle continues. Fig.3(e) shows the circuit diagram representation of this mode.

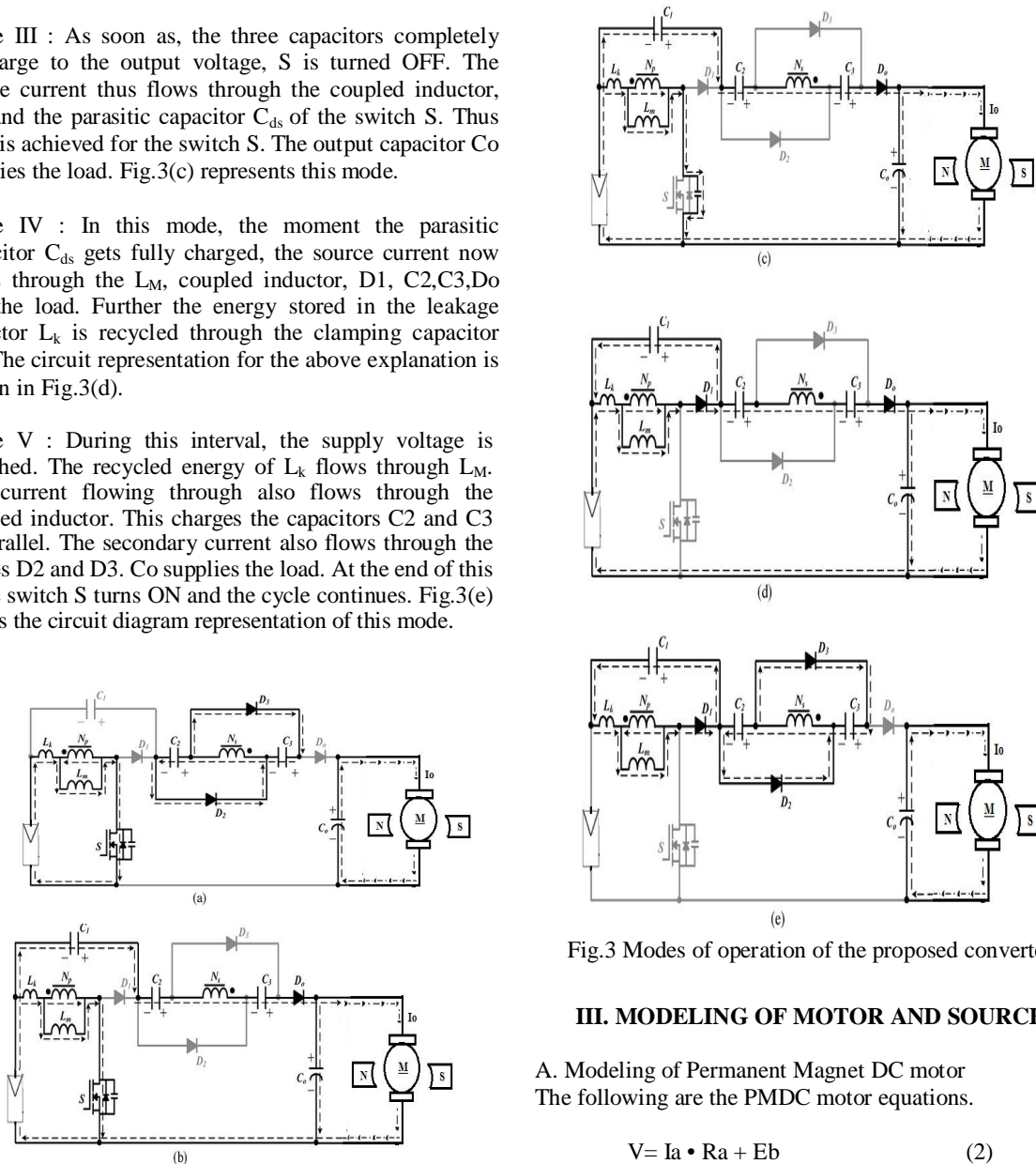


Fig.3 Modes of operation of the proposed converter

III. MODELING OF MOTOR AND SOURCE

A. Modeling of Permanent Magnet DC motor

The following are the PMDC motor equations.

$$V = I_a \cdot R_a + E_b \quad (2)$$

$$E_b = k \cdot \omega \quad (3)$$

$$\omega = 2 \cdot \pi \cdot n \quad (4)$$

$$\text{Torque Generation (Te)} = k \cdot I \quad (5)$$

where,

E_b - voltage induced in windings (back-EMF)

ω - Angular speed

Factor k depends on motor design features (number of winding turns, permanent magnet strength, air gap distance, rotor diameter, rotor length). The PMDC motor directly provides rotary motion and, coupled with wheels or drums and cables, can provide translational motion. The electric circuit of the armature and the free body diagram of the rotor are shown in the following Fig.4.1

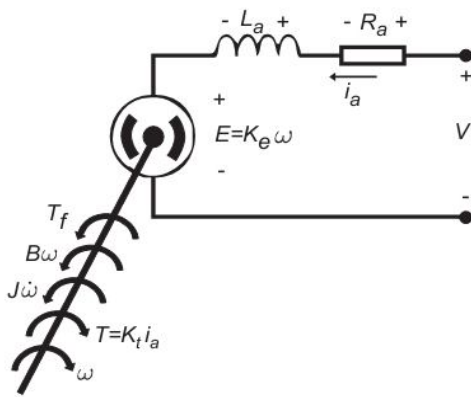


Fig.4.1 Circuit Model of PMDC motor

The motor torque, T, is related to the armature current, ia, by a constant factor Kt. The back emf, E, is related to the rotational velocity by the constant factor Ke as in the following equations:

$$T = K_t \cdot i_a \quad (6)$$

$$E = K_e \cdot \omega \quad (7)$$

$$V = R_a \cdot i_a + L_a \frac{di_a}{dt} + K_e \omega \quad (8)$$

$$K_t i_a = J \frac{d\omega}{dt} + B_m \omega + T \quad (9)$$

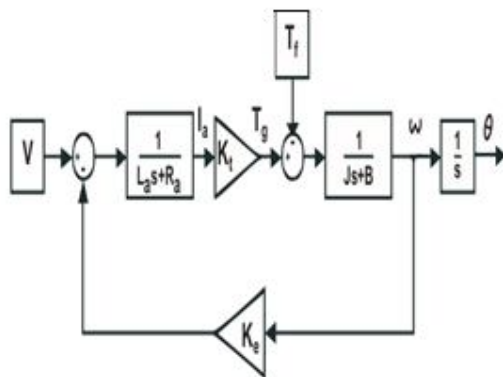


Fig.4.2 Modeling of PMDC motor

The modeling of the PMDC motor is drawn using the above equations as shown in Fig.4.2.

B. Modeling of Photovoltaic array system

The PV panel module physically moves to point directly at the sun and which the MPPT is not a mechanical tracking system. The battery is directly connected to the module and it is charging a discharged battery. Hence the module will be operated at battery voltage. The equivalent circuit of the PV cell is shown below in

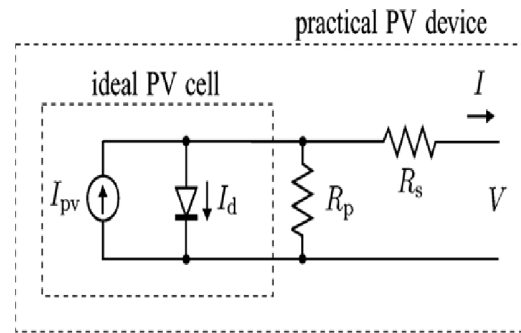


Fig.5.1,

Fig.5.1 Equivalent circuit of PV cell

The basic equation of I – V characteristic of the ideal PV is mathematically described from the theory of semiconductors

$$I = I_{pv,cell} - I_d \quad (10)$$

$$I_d = I_{o,cell} [\exp(qv/akt)] - 1 \quad (11)$$

therefore,

$$I = I_{pv,cell} - I_{o,cell} [\exp(qv/akt)] - 1 \quad (12)$$

where,

- $I_{pv,cell}$ is the current generated by the incident light (it is directly proportional to the Sun irradiation),
- I_d is the Shockley diode equation,
- $I_{o,cell}$ is the reverse saturation or leakage current of the diode, q is the electron charge ($1.60217646 \times 10^{-19}$ C),
- k is the Boltzmann constant ($1.3806503 \times 10^{-23}$ J/K), T (in Kelvin) is the temperature of the p-n junction, and a is the diode ideality constant.

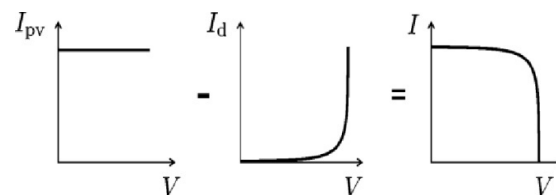


Fig.5.2 Origin of I -V equation of an Ideal PV cell

The Fig.5.2 shows the origination of the I – V curve for the equation (12). Practical arrays are made up of multiple modules. The observation of the characteristics at the terminals of the PV array requires the inclusion of additional parameters to the basic equation.

$$I = I_{pv} - I_0[\exp(V + R_s I)/V_t \alpha - 1] - (V + R_s I)/R_p \quad (13)$$

where,

$V = N_s kT/q$ is the thermal voltage of the array with N_s cells connected in series.

R_s & R_p is the equivalent series and parallel resistance of the array. The cells connected in parallel which increases the current and the greater output voltage will be produced by the cells connected in series. The N_p parallel connections of cell composes the array, the PV and saturation currents may be expressed as,

$$I_{pv} = I_{pv,cell} * N_p \quad (14)$$

$$I_0 = I_{0,cell} * N_p \quad (15)$$

C. Design of circuit parameters

$$L_m = f_s \cdot \frac{D^3 - 2D^2 + D}{2n^2 + 4n + 2} \quad (16)$$

$$V_{DS} = V_{D1} = \frac{V_{in}}{1 - D} \quad (17)$$

$$V_{D2} = V_{D3} = V_{D0} = \frac{n V_{in}}{1 - D} \quad (18)$$

Where,

D – Duty cycle

L_m – Magnetizing inductance

IV. TRIANGULAR PULSE WIDTH MODULATION

The magnitude of the dc modulating signal is constrained to remain between the minimum and maximum magnitudes of the triangular carrier signal. Now, the high frequency triangular carrier waveform is compared with the dc modulating signal and the comparator output is used to control the switch. The Fig.6 shown below explains the triangular PWM generation.

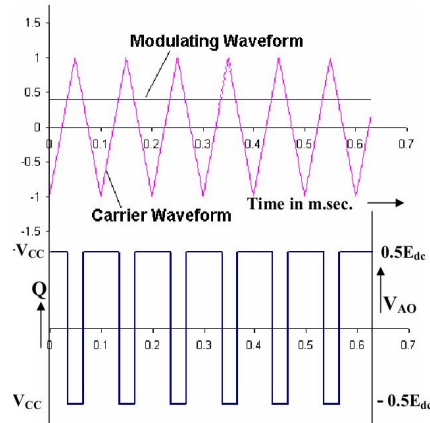


Fig. 5 Triangular Pulse Width Modulation generation

V. DISCUSSION OF SIMULATION RESULTS

The performance of the proposed converter is illustrated using PMDC motor load. The performance is studied by using Matlab simulation. The simulink model of the proposed converter with the PMDC motor load are shown in Fig.6.1 and Fig.6.2 respectively.

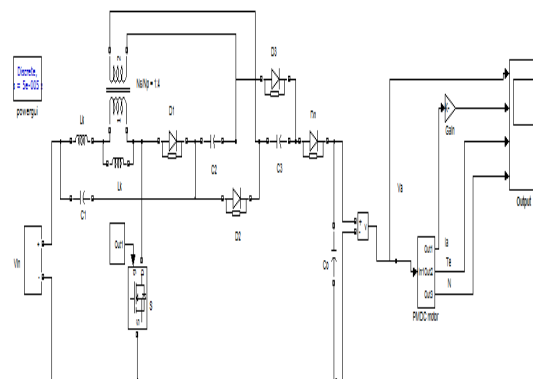


Fig.6.1 Simulink model

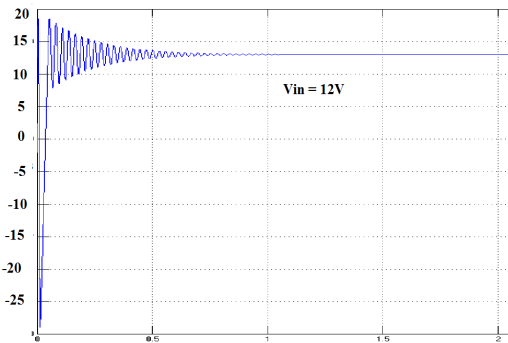


Fig.6.2 Input Voltage

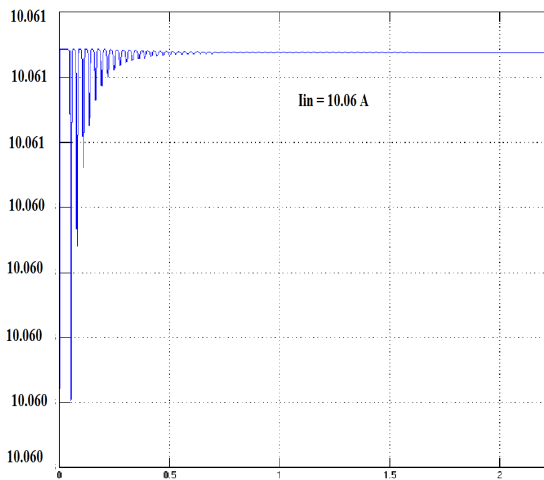


Fig.6.3 Input Current

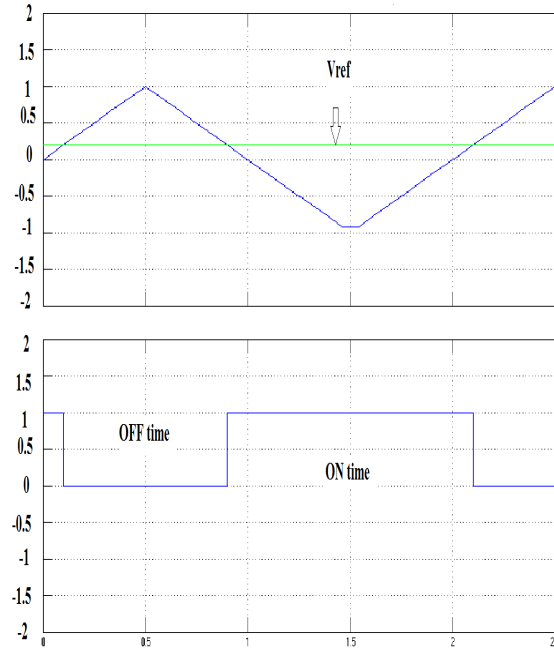


Fig.6.4 Pulse Generation

The resultant armature voltage, armature current and torque is shown if Fig.6.5,6.6 and 6.8 respectively. Pulses for the gate generated using triangular pulse width modulation technique are shown in Fig 6.4. A 0.5 HP, 1640 rpm PMDC motor is driven by using a 12 V solar panel. The armature voltage and the current obtained are from this proposed system are 100V, 5 A.

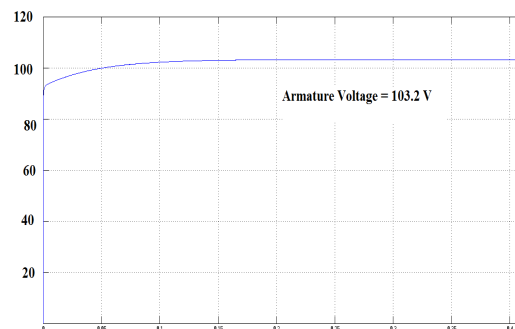


Fig.6.5 Armature Voltage

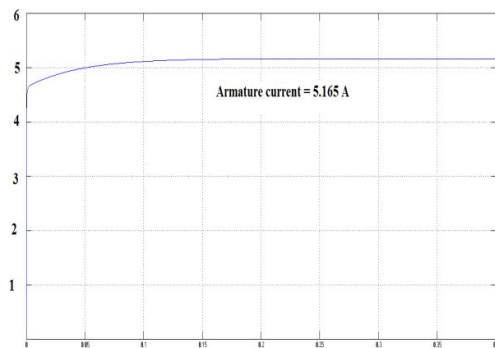


Fig.6.6 Armature current

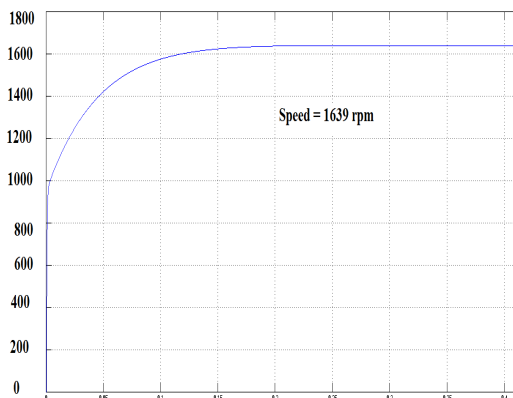


Fig.6.7 Speed

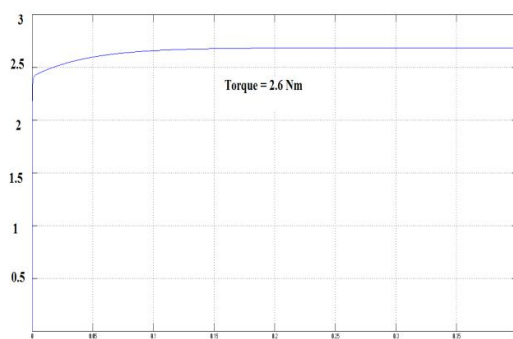


Fig.6.8 Torque

VI. CONCLUSION

The performance of the DC/DC converter is improved in this paper by effectively utilizing the energy stored in the passive elements. This converter is powered by the renewable of energy i.e. solar. The proposed system can be efficiently utilized in high speed drive applications. In this case, the proposed system is made to drive a PMDC

motor load. The converter receives an input voltage of 12V from the solar panel, and in turn produces 100V/ 5A driving a PMDC motor load of 0.5 rating. Further, soft switching technique with Triangular pulse width modulation strategy reduces the switching losses and stress thereby improving the efficiency further. Moreover as the energy stored in the passive elements are effectively utilized, the overall losses reduces considerably there adding the efficiency percentage. And also this proposed system is cost effective and can be used in wide range of drive applications.

REFERENCES

- [1] T. F. Wu, Y. S. Lai, J. C. Hung, and Y. M. Chen, "Boost converter with coupled inductors and buck-boost type of active clamp," IEEE Trans. Ind. Electron., vol. 55, no. 1, pp. 154–162, Jan. 2008.
- [2] R. J. Wai and R. Y. Duan, "High step-up converter with coupled-inductor," IEEE Trans. Power Electron., vol. 20, no. 5, pp. 1025–1035, Sep. 2005.
- [3] L. S. Yang, T. J. Liang, and J. F. Chen, "Transformerless dc-dc converter with high voltage gain," IEEE Trans. Ind. Electron., vol. 56, no. 8, pp. 3144–3152, Aug. 2009.
- [4] N. P. Papanikolaou and 4. E. C. Tatakis, "Active voltage clamp in fly back converters operating in CCM mode under wide load variation," IEEE Trans. Ind. Electron., vol. 51, no. 3, pp. 632–640, Jun. 2004.
- [5] R. J. Wai and R. Y. Duan, "High-efficiency dc/dc converter with high voltage gain," Proc. Inst. Elect. Eng.—Elect. Power Appl., vol. 152, no. 4, pp. 793–802, Jul. 2005.
- [6] Q. Zhao and F. C. Lee, "High-efficiency, high step-up dc-dc converters," IEEE Trans. Power Electron., vol. 18, no. 1, pp. 65–73, Jan. 2003.
- [7] O. Abutbul, A. Gherlitz, Y. Berkovich, and A. Ioinovici, "Step-up switching-mode converter with high voltage gain using a switched-capacitor circuit," IEEE Trans. Circuits Syst. I, Fundam. Theory Appl., vol. 50, no. 8, pp. 1098–1102, Aug. 2003.
- [8] M. G. Guerreiro, D. Foito, and A. Cordeiro, "A Sensorless PMDC Motor Speed Controller with a Logical Overcurrent Protection", Journal of Power Electronics, Vol. 13, No. 3, May 2013
- [9] Nobuyoshi Mutoh, Masahiro Ohno, and Takayoshi Inoue, "A Method for MPPT Control While searching for Parameters Corresponding to Weather Conditions for PV Generation Systems", IEEE TRANSACTIONS ON INDUSTRIAL ELECTRONICS, VOL. 53, NO. 4, AUGUST 2006.
- [10] Nicola Femia, Giovanni Petrone, Giovanni Spagnuolo and Massimo Vitelli, "Optimization of Perturb and Observe Maximum Power Point Tracking Method", IEEE TRANSACTIONS ON POWER ELECTRONICS, VOL. 20, NO. 4, JULY 2005.
- [11] Oscar López-Lapeña, María Teresa Penella and Manel Gasulla, "A New MPPT Method for Low-Power Solar Energy Harvesting", IEEE TRANSACTIONS ON INDUSTRIAL ELECTRONICS, VOL. 57, NO. 9, SEPTEMBER 2010.